Published in final edited form as:
Development. 2008 April ; 135(8): 1395–1405. doi:10.1242/dev.018945.

The apical ectodermal ridge is a timer for generating distal limb progenitors

Pengfei Lu*, **Ying Yu**, **Yasmine Perdue**, and **Zena Werb***
Department of Anatomy and Program in Developmental Biology, University of California at San Francisco, San Francisco, CA 94143-0452, USA

Abstract

The apical ectodermal ridge (AER) is a transient embryonic structure essential for the induction, patterning and outgrowth of the vertebrate limb. However, the mechanism of AER function in limb skeletal patterning has remained unclear. In this study, we genetically ablated the AER by conditionally removing FGFR2 function and found that distal limb development failed in mutant mice. We showed that FGFR2 promotes survival of AER cells and interacts with Wnt/β-catenin signaling during AER maintenance. Interestingly, cell proliferation and survival were not significantly reduced in the distal mesenchyme of mutant limb buds. We established *Hoxa13* expression as an early marker of distal limb progenitors and discovered a dynamic morphogenetic process of distal limb development. We found that premature AER loss in mutant limb buds delayed generation of autopod progenitors, which in turn failed to reach a threshold number required to form a normal autopod. Taken together, we have uncovered a novel mechanism, whereby the AER regulates the number of autopod progenitors by determining the onset of their generation.

Keywords

Apoptosis; Autopod progenitors; Cell proliferation; FGF signaling; Limb patterning; Mouse; Wnt signaling

INTRODUCTION

The apical ectodermal ridge (AER) is an essential signaling center governing vertebrate limb development (Capdevila and Izpisua Belmonte, 2001; Martin, 1998; Niswander, 2003). The importance of the AER was demonstrated by classic experiments in chicken embryos showing that AER removal at progressively later stages of limb development causes a progressive loss of distal elements of the limb (Saunders, 1948; Summerbell, 1974). Although different models have been proposed to explain limb skeletal patterning along the proximal-distal (PD) axis, AER function in this process has remained largely unclear. For example, the Progress Zone (PZ) model postulates that the AER provides permissive signals to keep PZ cells labile until they exit the zone, at which time these cells are autonomously specified by ceasing to acquire ‘positional information’ (Summerbell et al., 1973). By contrast, the Early Specification (ES) model proposes that PD elements are specified, rather than progressive, at the earliest stages of limb bud development and that the AER regulates subsequent expansion of progenitor pools by promoting cell proliferation and survival (Dudley et al., 2002). Furthermore, recent models suggest that PD elements are specified via dynamic interactions between the flank of the lateral plate mesoderm and the AER (Mercader et al., 2000; Tabin and Wolpert, 2007).

*Authors for correspondence (e-mail: pengfei.lu@ucsf.edu, zena.werb@ucsf.edu).

A transient structure, the AER undergoes a series of morphogenetic changes consisting of four stages – initiation, maturation, maintenance and regression – each characterized by distinctive changes of cell shape and gene expression (Altabef et al., 1997; Kimmel et al., 2000). Briefly, AER initiation in the mouse forelimb starts at approximately embryonic day (E) 9, when the limb bud is first discernable and the gene expression in the ventral ectoderm that marks the future AER becomes apparent. During AER maturation, pre-AER cells in the ventral ectoderm migrate towards the distal tip and undergo a compaction process, whereby a distinctive narrow band of stratified columnar epithelium forms at ~E10 (Loomis et al., 1998). The mature AER is then maintained for an additional 2–3 days, while mesenchymal skeletal progenitors continue to proliferate and differentiate until a fully patterned limb emerges. The AER then regresses via programmed cell death and eventually flattens to a simple cuboidal epithelium (Guo et al., 2003).

At the molecular level, AER initiation involves interactions of several major signaling pathways. The prevailing model holds that Wnt2b-Wnt8c/β-catenin signaling in the lateral plate mesoderm is required for *Fgf10* expression in the presumptive limb bud mesenchyme (LBM) (Kawakami et al., 2001), which in turn regulates Wnt3/β-catenin signaling in the overlying ectoderm to induce AER formation (Barrow et al., 2003; Kengaku et al., 1998). BMP signaling also plays a role in this process, as mice lacking *Bmpr1a* in the ectoderm fail to form the AER (Ahn et al., 2001). The molecular basis of the remaining stages of AER morphogenesis is less clear. Studies have shown, however, that engrailed 1 (*En1*) plays a role during migration and compaction of AER progenitor cells (Loomis et al., 1998), whereas Wnt/β-catenin signaling is required to maintain the AER after AER initiation and maturation (Barrow et al., 2003). By contrast, BMP signaling promotes destruction of the AER during the regression process (Pizette and Niswander, 1999), despite its early role in initiating the AER.

FGFR2 functions in both limb ectoderm and mesenchyme during limb development (Itoh and Ornitz, 2004). Although mouse embryos completely lacking *Fgfr2* function fail to develop beyond implantation stages (Arman et al., 1998), those with partial loss of *Fgfr2* function, including ones specifically lacking the 2b isoform (De Moerlooze et al., 2000; Revest et al., 2001), survive to later embryonic stages, but fail to develop limbs (Arman et al., 1999; Gorivodsky and Lonai, 2003; Xu et al., 1998). These results suggest that AER initiation requires ectodermal FGFR2 function to respond to mesenchymal FGF10 signaling, as mice lacking mesenchymal *Fgf10* are also limbless (Min et al., 1998; Sekine et al., 1999). However, mesenchymal expression of FGFR2 (Coumoul et al., 2005), as well as of FGFR1 (Li et al., 2005; Verheyden et al., 2005), is essential for skeletal progenitor cells to respond to AER-FGFs to ensure normal skeletal formation and patterning. In this study, we used a conditional approach based on the Cre/*lox* system to modify the AER. We found that AER maintenance requires FGFR2 function and is essential for distal limb development.

MATERIALS AND METHODS

Mouse strains

Mice carrying a conditional *Fgfr2* null allele, $Fgfr2^{fl}$ (Yu et al., 2003), the *Msx2-cre* transgene (Lewandoski et al., 2000) or a conditional gain-of-function (GOF) allele of *β-catenin*, $Catnb^{lox(ex3)}$ (Harada et al., 1999) were kindly provided by Drs David Ornitz, Gail Martin and Makoto Mark Taketo, respectively. Mice carrying the BAT-Gal transgene, a reporter of Wnt/β-catenin signaling activities (Maretto et al., 2003), were purchased from the Jackson Laboratory (Stock #005317). All mice were maintained on a mixed genetic background and genotyped based on previously published reports.

Phenotypic analysis

Noon of the day when a vaginal plug was detected was considered ~E0.5. Embryos were collected in cold PBS, fixed in 4% paraformaldehyde (PFA), and stored in 100% methanol at −20°C. To stage embryos more precisely, the somites posterior to the forelimb bud were counted and the total number of somites was determined by scoring the first one counted as somite 13. Each somite stage is ~2 hours. E10.5 is equivalent to ~35-sominte stage and E11.5 is equivalent to ~45-somite stage. Standard protocols were used for RNA in situ hybridization and skeletal preparations as previously described (Lu et al., 2006). The area of *Hoxa13* expression was measured using ImageJ. β-galactosidase (β-Gal) activity was conducted using standard protocol. Bright-field images were captured with a Leica DMR HC microscope using a 40×/0.75 Plan Apochromat air objective.

Immunofluorescence, cell proliferation and cell death analyses

Embryos were embedded in agarose, and 40 μm sections were cut using a Leica vibratome. Samples were blocked in PBS containing 5% BSA and 0.5% Tween 20 for 1 hour before they were subjected to incubation with primary antibodies, anti-β-catenin mAb (BD-Biosciences), anti-CD44 (BD-Biosciences) and anti-phospho-Histone H3 (pH3, Upstate Biotechnology). Goat-anti-rabbit secondary antibodies (AlexaFluor488, Invitrogen) were used to detect the primary antibodies.

Cell proliferation analyses were based on either detection of 5-bromodeoxyuridine (BrdU) incorporation or pH3 immunofluorescence, which marks nuclei in cells undergoing mitosis. For BrdU analysis, mice were injected with BrdU (5 mg/100 g body-weight) 1 hour prior to euthanasia. Embryos were harvested and fixed in 4% PFA. Transverse paraffin sections (5 μm) were cut using microtome and five sections, 50 μm apart from the middle region of each limb bud were used for BrdU detection. Antigen was retrieved in 10 mM sodium citrate (pH 6.0) in a microwave oven and BrdU was detected using a kit from Roche (Cat#1296736). Alternatively, 40 μm vibratome sections were used for pH3 immunofluorescence. All samples were counterstained with To-Pro-3 (Invitrogen). The total number of nuclei and BrdU-positive nuclei or pH3-positive nuclei in a 3.1×10^4 μm^2 area (ϕ=200 μm) of the sub-AER limb mesenchyme were counted in each section. BrdU incorporation and pH3 immunofluorescence were quantified using ImageJ. Confocal microscopy was performed on a ZeissLSM510 confocal.

Assays for cell death via TdT-mediated dUTP nick-end-labeling (TUNEL) analysis on vibratome sections were performed according to manufacturer's protocol (Roche Cat#1684817), while those via LysoTracker (MolecularProbesL-7528) staining were conducted as previously reported (Lu et al., 2006). A total of over 180 embryos were examined between the 28- and 45-somite stages by TUNEL or Lysotracker staining (at least five mutant embryos were examined for each stage).

RESULTS

AER maintenance is required for later stages of mouse forelimb development

The *Msx2-cre* transgene expresses *cre* in the ventral ectoderm and the AER of early limb buds (Lu et al., 2006; Sun et al., 2000). Importantly, in the hindlimb *Msx2-cre* acts before limb bud induction, while in the forelimb *cre* is not expressed until ~20 hours after AER initiation (Sun et al., 2002). We crossed male mice homozygous for the *Msx2-cre* transgene and heterozygous for the *Fgfr2*-null allele, $Fgfr2^{\Delta}$ (Yu et al., 2003), with female mice homozygous for the *Fgfr2* conditional allele, $Fgfr2^{fl}$ (Yu et al., 2003). All *Msx2-cre;*$Fgfr2^{fl/\Delta}$ progeny ($Fgfr2^{AER\text{-}KO}$) were viable and displayed anomalies, including hair overgrowth (not shown), when compared with their morphologically normal 'control' littermates (*Msx2-cre;*$Fgfr2^{fl/+}$).

We found that *Fgfr2* removal via *Msx2-cre* before AER initiation eliminated the hindlimb of *Fgfr2*$^{AER-KO}$ embryos at E18.5 (Fig. 1A, B; *n*=18). By contrast, *Fgfr2* removal at the 26- to 28-somite (s) stage after AER initiation in the forelimb eliminated only distal bones (Fig. 1C–F). In these mutants, although the humerus, radius and ulna were present and of normal sizes, the autopod (hand-plate) was absent except for a few carpal bones (Fig. 1C–F, *n*=18). Thus, FGFR2 is required for later stages of mouse forelimb development.

The loss of distal elements in *Fgfr2*$^{AER-KO}$ forelimbs resembles the limb truncations of chicken embryos in AER removal studies (Saunders, 1948; Summerbell, 1974). To determine whether the AER is maintained in mutant forelimb buds, we examined the histological and molecular consequences of FGFR2 removal during AER morphogenesis. AER histology was assessed by the immunofluorescence of CD44, an AER marker (Sherman et al., 1998), on vibratome sections of early limb buds at stages after *cre* activation. In control embryos, we noted a distinctive AER composed of stratified epithelium at the 29 s stage, which became progressively more compact along the dorsal-ventral (DV) axis at later stages (33–45s) (Fig. 1G, I, K, M). In mutant limb buds, the AER was also distinctive at the 29 s stage, although it was slightly thinner than normal (Fig. 1H). During later stages, the mutant AER became progressively thinner and did not compact along the DV axis (Fig. 1J, L). By the 45 s stage, the AER in mutant limb buds was lost, as shown by the lack of stratified epithelium in limb ectoderm and the absence of CD44 expression (Fig. 1N). The loss of the AER was also shown by the lack of expression of additional AER markers, including *Bmp4*, *Dlx2*, *Sp8* and *En1*, in mutant limb buds at E11.5 (not shown). Thus, FGFR2 is required for AER maintenance during mouse limb development.

We then analyzed how expression of *Fgf8*, the primary AER-*Fgf* mediating AER function (Lewandoski et al., 2000; Moon and Capecchi, 2000), is affected by premature AER loss. Using RNA in situ hybridization on whole-mount embryos, we found that *Fgf8* was expressed at a relatively normal level in mutant limb buds at the 28-somite stage (Fig. 1O–P′). However, by the 33-somite stage, *Fgf8* expression was noticeably less in mutant limb buds than in control (Fig. 1Q–R′). Moreover, *Fgf8* expression became discontinuous, and gaps lacking *Fgf8* expression were often observed in mutant limb buds at later stages, including the 35 s (not shown) and 39 s stages (Fig. 1S–T′). By the 45 s stage, *Fgf8* expression was essentially absent, except occasionally in a tiny patch of the residual AER (Fig. 1V). No *Fgf8* expression was observed afterwards (not shown). Thus, FGFR2 removal causes premature AER regression and progressive AER-FGF reduction.

Expression of key mesenchymal patterning genes is altered when the AER fails to be maintained

To determine how the mesenchymal gene expression is affected, we examined *Mkp3* expression, a downstream target of FGF signaling (Kawakami et al., 2003). We found that *Mkp3* expression was not obviously different in *Fgfr2*$^{AER-KO}$ and control forelimb buds at the 27 s (not shown) or 30 s stage (Fig. 2A, B). However, the *Mkp3* expression domain was reduced by the 32 s stage in mutant limb buds (Fig. 2C, D) and became progressively smaller at later stages (Fig. 2E–H). By the 46 s stage, while the proximal domain of *Mkp3* expression was not affected, the *Mkp3*-positive domain in the sub-AER mesenchyme was absent (Fig. 2G, H) because the distal limb bud failed to form in mutant limbs (see below). The *Mkp3* expression domain was also lacking in the distal mesenchyme of mutant limbs at E12.5, when extensive *Mkp3* expression was evident in the autopod of control limb buds (not shown). Thus, FGF signaling activities continuously decrease in mutant limb buds.

AER-FGFs influence limb mesenchyme in part via a positive-feedback loop involving *Shh* and its downstream target *Gremlin* (*Gre*). We found that at the 35 s stage *Shh* expression in the mutant was not significantly different from that in control limb buds (Fig. 2I, J), but that at

E11.5 its expression domain was smaller than control in mutant limb buds (Fig. 2K, L). Likewise, *Gre* expression was not greatly changed at E10.5 (not shown) but its expression domain was significantly reduced by E11.5 (Fig. 2M–N′). Moreover, the thin strip of *Gre*-negative cells in the sub-AER mesenchyme or the mid-section along the DV axis was absent in mutant limb buds by E11.5 (Fig. 2M–N′). Thus, *Shh* and *Gre* expression domains are reduced as a result of decreasing AER-FGF signaling activities.

In addition, we found that expression of *Alx4*, *Meis2* and *Hoxa11*, markers for the anterior mesenchyme (Fig. 2O), the proximal mesenchyme (Fig. 2Q), and the slightly more distal mesenchyme (Fig. 2S), respectively, was not changed in mutant limb buds at E11.5 (Fig. 2P, R, T). Likewise, the proximal domain of *Hoxd11* expression, which marks the proximal mesenchyme, was not affected in mutant limb buds (Fig. 2U, V). By contrast, the distal domain of *Hoxd11* expression, which marks the future autopod (Tarchini and Duboule, 2006) (see below), was completely absent in mutant limb buds at E11.5 (Fig. 2U, V). As *Hoxd11* expression in these two domains results from two separate transcriptional events, first in the proximal then in the distal mesenchyme (Tarchini and Duboule, 2006), the lack of *Hoxd11* expression in the distal domain could be due to either delayed transcription in the distal mesenchyme or an absence of the future autopod. No *Hoxd11* expression in the distal domain was observed at E12.5 (not shown), thus arguing against the possibility of a transcriptional delay of *Hoxd11*. These data suggest that the molecular events causing loss of the distal autopod in mutant embryos have occurred by E11.5.

Loss of the distal autopod in mutant limbs is unlikely due to abnormal cell death or proliferation in the distal limb bud mesenchyme

What events might cause loss of the distal autopod in $Fgfr2^{\text{AER-KO}}$ embryos? There are two obvious possibilities, e.g. increased cell death and decreased cell proliferation in the distal mesenchyme, either or both could reduce the pool of autopod progenitors in mutant limb buds. First, we examined cell death in mutant limb buds at every somite stage between the 28 s and 45 s (E11.5) stages (at least five mutant embryos were examined for each stage) by TUNEL or Lysotracker staining. However, we did not observe abnormal cell death in the distal mesenchyme at these stages (Fig. 3A–D, not shown). Therefore, loss of the distal autopod in mutant forelimbs is unlikely to be due to death of autopod progenitors in the distal mesenchyme. Interestingly, we found that the number of dying cells in the AER and ventral ectoderm, where both *Msx2-cre* (Lu et al., 2006) and *Fgfr2* (Arman et al., 1999; Min et al., 1998; Revest et al., 2001) are expressed, was greater in mutant forelimb buds than in control limb buds at the 30 s stage (Fig. 3A, B; n=8). A similar pattern of cell death was observed in mutant limb buds up to the 36 s stage (Fig. 3C, D; n=6), when AER morphology was no longer distinct. Thus, FGFR2 acts as a survival factor to maintain the AER and, in its absence, the AER regresses prematurely owing to increased cell death.

Next, we examined cell proliferation in mutant limb buds by assaying the percentage of cells in an area [3.1×10^4 μm^2, approximately the size of the hypothetical PZ (Dudley et al., 2002; Summerbell et al., 1973)] of the sub-AER mesenchyme that incorporated BrdU after a 1-hour pulse. We found no significant differences between the percentages of BrdU-positive cells in the distal mesenchyme of mutant and control limb buds either at the 34 s or 44 s stage (Fig. 3E–H′, M). We also examined the mitotic index as indicated by pH3 immunofluorescence in the sub-AER mesenchyme but again found no significant differences between mutant and control limb buds at the 36 s, 39 s or E11.5 stages (Fig. 3I–L, N). Thus, based on two independent methods, our results indicate that global reduced cell proliferation is unlikely to account for loss of the distal autopod in mutant limbs.

Hoxa13 expression is an early marker of distal limb progenitors

A third possibility to explain loss of the distal autopod in *Fgfr2*$^{AER-KO}$ embryos is that the early events of autopod progenitor formation may be compromised when the AER prematurely regresses in mutant limb buds. Consequently, a reduced number of autopod progenitors may be generated, which may be able to proliferate and expand similarly as those in control limb buds but fail to produce a sufficient number of skeletal progenitors required to form normal autopod elements. To test this possibility, we first reanalyzed several *Hox* genes, including *Hoxd11*, *Hoxd13* and *Hoxa13*, that are known to be expressed in the autopod at late stages as potentially useful markers of early autopod progenitors. As shown previously, *Hoxd11* was expressed in the distal autopod at E12.5 (Fig. 4C); however, this distal domain of *Hoxd11* expression arose between E10.5 (Fig. 4A) and the 40 s stage (E11.0; Fig. 4B). Thus, *Hoxd11* expression at E10.5 probably marks progenitors of both the proximal limb and the autopod. Unlike *Hoxd11*, *Hoxd13* expression was confined to the distal autopod at E12.5 (Fig. 5O). However, at the 34–35 s stage, *Hoxd13* was also expressed in the posterior-proximal limb bud (Fig. 4D). This proximal domain of *Hoxd13* expression was gradually reduced as the limb bud grew out (Fig. 4E, Fig. 5M, not shown) and was lost after the ~49 s stage (Fig. 4F, Fig. 5O). Thus, *Hoxd13* expression at E10.5 is also likely to mark progenitors of both the proximal limb and the autopod.

Hoxa13 was expressed only in the distal autopod as *Hoxd13* at E12.5 (Fig. 5K). Unlike *Hoxd13*, however, *Hoxa13* was not expressed in the proximal limb bud at the 35 s stage (Fig. 4G). Rather, at this stage, it was expressed in a thin strip of the posterior-distal mesenchyme, correlating with the area that is going to give rise to the future autopod based on fate-mapping studies of the chicken limb buds at the equivalent stages (Sato et al., 2007;Vargesson et al., 1997). Looking more closely over time, we found that *Hoxa13* was first expressed in the posterior-distal mesenchyme in forelimb buds at the 31–32 s stages (Fig. 5A). As the limb bud grew out at later stages, the *Hoxa13*-positive domain expanded concomitantly and extended anteriorly until a well-patterned limb emerged at E12.5 (Fig. 4G–I; Fig. 5C, E, G, I, K, U, U ′). Importantly, we have never observed a loss of expression domain for *Hoxa13*, as we did for *Hoxd13*, during the course of early limb bud development, suggesting that *Hoxa13* expression is unlikely to mark progenitors of the proximal mesenchyme. Thus, consistent with studies showing that *Hoxa13* is initially expressed in a subpopulation of autopod progenitors (Nelson et al., 1996;Sato et al., 2007), our data suggest that *Hoxa13* expression in the early limb bud marks autopod progenitors of the distal limb.

Generation of autopod progenitors is delayed in mutant limb buds

Next, we examined development of autopod progenitors by analyzing *Hoxa13* expression in mutant limb buds. We found that the onset of *Hoxa13* expression was delayed by two somite stages beginning at the 33–34 s stages instead of at the 31–32 s stages in *Fgfr2*$^{AER-KO}$ limb buds (Fig. 5C, D; Table 1). At later stages, the *Hoxa13* expression domain expanded at a relatively stable pace, as in the control. Thus, at the stages examined after its initiation, the area of the *Hoxa13*-expression domain in the mutant was ~45% of that in the control until about the 45 s stage, when it reached a plateau and barely expanded afterwards (Fig. 5F, H, J, L, U, U′). *Hoxd13* expression, marking slightly more distal autopod, confirmed that autopod expansion was indeed stalled by the 47 s and E12.5 stages (Fig. 5M–P).

Interestingly, the outline of the mutant limb bud, which was smooth and regular at the 45 s stage (Fig. 5H), became rugged and irregular by the 47 s stage (Fig. 5J). These changes of limb bud shape may reflect ongoing cellular events, e.g. chondrocyte condensation of the autopod in the underlying mesenchyme. To test this possibility, we examined *Sox9* expression to directly visualize skeletal progenitors in early limb buds. We found that at the 40 s stage, when skeletal condensation had yet to start, the total number of skeletal progenitors was not grossly

different between mutant and control limb buds (Fig. 5Q, R). By the 46 s stage, skeletal condensation had occurred, and although stylopod and zeugopod rudiments in mutant forelimb buds appeared normal (Fig. 5S, T), autopod rudiments were absent. Thus, consistent with previous studies suggesting that skeletal condensation occurs on a fixed schedule in a proximal to distal wave, our data indicate that the autopod progenitor pool in mutant limb buds is insufficient, owing to delayed generation and expansion, to form a normal autopod at the onset of autopod condensation.

Wnt/β-catenin and FGFR2 signaling interact to maintain the AER

To examine whether Wnt/β-catenin signaling is affected by *Fgfr2* removal, we used the reporter allele of the BAT-Gal transgene to directly examine Wnt/β-catenin signaling (Maretto et al., 2003). We found that Wnt/β-catenin signaling was greatly reduced in the AER of *Fgfr2*$^{\text{AER-KO}}$ forelimb buds at the 33 s stage (Fig. 6A, *n*=6; Fig. 6B, *n*=4), although ectopic activities was also observed in the distal-dorsal mesenchyme (Fig. 6B, arrow). In addition, expression of *Lef1*, which plays a role in limb development (Galceran et al., 1999), was reduced in mutant limb buds than in control at E10.5 (~35 s stage) (Fig. 6C, D). *Tcf1* and *Wnt3* expression were not significantly changed (not shown). Thus, FGFR2 is required for normal Wnt/β-catenin signaling during AER maintenance.

Next, we asked whether gain of Wnt/β-catenin signaling in the AER may prevent premature AER loss and restore autopod bones in the mutant limb. We crossed male mice homozygous for the *Msx2-cre* transgene and heterozygous for the *Fgfr2*$^{\Delta}$ allele with female mice homozygous for the *Fgfr2*$^{\text{fl}}$ allele and heterozygous for the *Catnb*$^{\text{lox(ex3)}}$ allele, a conditional GOF allele of *β-catenin* (Harada et al., 1999), to generate *Msx2-cre;Fgfr2*$^{\text{fl/}\Delta}$;*Catnb*$^{\text{lox(ex3)}}$ embryos (referred to as *Fgfr2*$^{\text{AER-KO}}$*; β-cat*$^{\text{GOF}}$ hereafter). In these embryos, *Msx2-cre*-mediated recombination inactivates *Fgfr2* by converting *Fgfr2*$^{\text{fl}}$ to a null allele and concomitantly activates *β-cat*$^{\text{GOF}}$ expression from the *Catnb*$^{\text{lox(ex3)}}$ conditional allele. We found that β-catenin overexpression (Fig. 6E–H) caused ectopic *Fgf8* expression in the ventral ectoderm at E11.75 (Fig. 6I, K), when it was already absent in the mutant limb bud (Fig. 1N, V; Fig. 6J). In *Fgfr2*$^{\text{AER-KO}}$*; β-cat*$^{\text{GOF}}$ limb buds, *Fgf8* expression was retained in the mutant AER and was ectopically expressed in the ventral ectoderm (Fig. 6L). Moreover, we found that β-catenin GOF prevented ectopic cell death in the ventral ectoderm (Fig. 6N, *n*=3) and restored normal expression of *Hoxa13* in mutant limb buds (Fig. 6O, P; Table 1). Furthermore, we found that the distal limb elements, based on *Sox9* expression marking skeletal progenitors (Fig. 6Q, R) and skeletal staining (Fig. 6T, *n*=5), were present in *Fgfr2*$^{\text{AER-KO}}$*; β-cat*$^{\text{GOF}}$ embryos. Together, these data showed that β-catenin GOF prevents AER loss and restores the autopod in *Fgfr2*$^{\text{AER-KO}}$ limb buds.

DISCUSSION

In this study, we ablated the AER by genetically removing FGFR2 function and demonstrated that AER maintenance is essential for distal limb development. We showed that FGFR2 promotes survival of AER cells and that it interacts with Wnt/β-catenin signaling during AER maintenance. Interestingly, we found that neither cell survival nor cell proliferation was affected in the distal mesenchyme of *Fgfr2*$^{\text{AER-KO}}$ forelimb buds. This is in contrast to the current model suggesting that the AER regulates limb skeletal progenitors by promoting cell survival and proliferation in the mesenchyme. To uncover the role of the AER in autopod development, we validated *Hoxa13* expression as a marker of autopod progenitors and described a dynamic morphogenetic process of autopod development. In mutant limb buds, generation of autopod progenitors was delayed, which in turn failed to reach a critical mass required to form a normal autopod. Thus, we have serendipitously discovered a novel

mechanism whereby the AER regulates the number of autopod progenitors by determining the onset of their generation.

Hoxa13 expression is an early marker of distal limb progenitors

There are several lines of evidence suggesting that *Hoxa13* expression is an early marker of autopod progenitors. First, the initial expression domain of *Hoxa13* resides in a thin strip of the posterior-distal mesenchyme at the 31–32 s stage, which is the area of the early limb bud shown by fate-mapping studies in the chick at comparable stages to give rise to the autopod (Sato et al., 2007; Vargesson et al., 1997). In addition, despite close examination, we never observed a loss of *Hoxa13* expression domain during early limb bud development. These results suggest that, in contrast to *Hoxd13*, the initial *Hoxa13* expression domain is unlikely to mark progenitors of the proximal limb. Indeed, studies have shown that this initial *Hoxa13* expression domain marks only a subpopulation of autopod progenitors. For example, using DiI labeling in chick embryos, Nelson and colleagues demonstrated that *Hoxa13*-positive cells in early limb buds ultimately give rise to only the posterior two-thirds of the autopod (Nelson et al., 1996). Likewise, recent studies suggested that this initial *Hoxa13* expression domain contributes to the distal ~two-thirds of the future autopod (Sato et al., 2007). The most anterior and proximal autopod progenitors, which express *Hoxa13* at E12.5, must acquire *Hoxa13* expression de novo, thus highlighting a heterogeneous origin of autopod progenitors.

By contrast, *Hoxd13*, which is ultimately expressed in the emerging autopod similar to *Hoxa13*, is initially expressed in a subpopulation of zeugopod progenitors. The domain of *Hoxd13* expression in the autopod, like that of *Hoxd11*, is the result of a second-wave transcriptional event controlled by an enhancer element shared by the *HoxD* family of genes (Tarchini and Duboule, 2006). Thus, the final pattern of *Hoxd13* expression in the autopod is a combined result of downregulation of its expression in the proximal domain and upregulation of its expression in the distal mesenchyme (Vargesson et al., 1997).

Based on data showing that AER removal in chicken limb buds at the stage 20/21 causes loss of *Hoxa13* expression, it was suggested that the AER directly regulates *Hoxa13* expression (Hashimoto et al., 1999; Vargesson et al., 2001). In light of recent studies (Dudley et al., 2002), an alternative explanation is that loss of *Hoxa13* expression may be caused by death of autopod progenitors because of AER removal. Indeed, our data show that *Hoxa13* expression is initiated, albeit with a delay, and its domain is able to expand in the presence of dwindling AER-FGF signaling activities. In addition, *Hoxa13* expression is maintained for at least 24 hours after the AER is lost and sub-AER mesenchymal FGF signaling is absent by the 45 s stage. Together, these results suggest that the AER indirectly regulates *Hoxa13* expression by directly controlling development of autopod progenitors (see below).

Generation of autopod progenitors requires normal AER function

Our data support a model in which the AER influences autopod development by regulating ‘generation’ (see below) of autopod progenitors (Fig. 7). Previous studies suggest that skeletal condensation occurs on a fixed schedule in a proximal to distal wave (Dudley et al., 2002;Lewandoski et al., 2000;Sun et al., 2002;Wolpert et al., 1979) (reviewed by Mariani and Martin, 2003). Thus, whether a normal autopod forms depends on the number of progenitors at the time of autopod condensation. In $Fgfr2^{\text{AER-KO}}$ limbs, the onset of generation of autopod progenitor is delayed by two somite stages because of premature AER regression and reduction of AER-FGF signaling activities in the LBM (Fig. 7B). This delay of progenitor generation causes an insufficient number of autopod progenitors to be available at autopod condensation to form normal autopod bones. Remarkably, autopod progenitors in mutant limbs are initially able to expand at a rate comparable with that in the control when AER-FGF signaling activities progressively diminish in the mesenchyme. These data thus suggest that the primary function

of the AER is to promote generation of autopod progenitors during vertebrate distal limb development.

There are several major distinctions between our model and the existing models, in particular the PZ model (Summerbell et al., 1973), the ES model (Dudley et al., 2002) and other recent models (Mercader et al., 2000; Tabin and Wolpert, 2007), regarding limb skeletal patterning along the PD axis. Unlike these models, which are concerned with and differ at when limb elements are specified, our model deals with events after the distal skeletal elements are specified. Indeed, *Hoxa13* is unlikely to specify the autopod directly, even though it is required for autopod development (Fromental-Ramain et al., 1996). At present, specification markers of the PD elements are still elusive. It is thus unclear precisely when and where the autopod is specified, how many progenitor cells are present in the initial pool, to what extent cell proliferation is involved and whether these earliest autopod progenitors share similar proliferative properties to cells in other parts of the mesenchyme. For the sake of simplicity and clarity in discussing our data, we have used the generic term ‘generation’ to distinguish these early events, which include autopod specification, of autopod progenitor development proceeding *Hoxa13* expression with the later ‘expansion’ event, which our data suggest is initially less sensitive to reduced FGF signaling activities.

To explain loss of distal elements in AER removal experiments, the PZ model proposes that, in the absence of the AER, PZ cells loss their lability, stop acquiring distal ‘positional information’ and fail to be specified as distal elements (Summerbell et al., 1973). By contrast, our data show that autopod progenitors in *Fgfr2*$^{\text{AER-KO}}$ forelimb buds express markers, including *Hoxd13* and *Hoxa13*, of events that occur after autopod specification. Our model suggests that the loss of the distal limb is due to an insufficiency of skeletal progenitors at the onset of autopod condensation, rather than to failure of specification according to the PZ model. Moreover, by regulating generation of AER progenitors, the AER may play more than a permissive role as the PZ model suggests. Finally, whereas the ES model proposes that the AER regulates skeletal progenitor pools by promoting cell proliferation and survival (Dudley et al., 2002), our model shows that, at least for the autopod, this is accomplished by controlling the number of progenitors that are initially generated.

It is noteworthy that our model provides new mechanistic insights on several puzzling skeletal phenotypes reported previously. For example, although mice lacking AER-*Fgf4*/*8* fail to form the hindlimb autopod, neither cell proliferation nor cell death is affected in the distal mesenchyme (Sun et al., 2002). In light of our results, it is possible that generation of autopod progenitors may be delayed, or prevented in these mutants. Furthermore, it remains possible that the AER, in addition to promoting survival of stylopod and zeugopod progenitors (Barrow et al., 2003; Dudley et al., 2002; Sun et al., 2002), may also regulate their generation. Consistent with this notion, mouse limb buds that lack *Fgf4*/*8*, which fail to form normal stylopod and zeugopod, are smaller than normal at the earliest stages of limb development without changes of cell death or cell proliferation in the mesenchyme (Sun et al., 2002).

Absence of abnormal cell death and cell proliferation in the distal mesenchyme

The lack of cell death in the distal mesenchyme of *Fgfr2*$^{\text{AER-KO}}$ forelimbs is consistent with results from previous studies. As mentioned, cell death is increased only in the proximal but not in the distal mesenchyme, where autopod progenitors reside, of embryos lacking AER-*Fgf4*/*8* (Sun et al., 2002). In addition, whereas AER removal before stage 24 in the chick [which eliminates proximal limb elements up to the wrist (Niswander et al., 1993)] causes cell death in the distal mesenchyme, AER removal after stage 25 (which results in loss of the distal autopod) does not (Dudley et al., 2002). It is interesting to note that, although abnormal cell death was observed in the limb bud mesenchyme of certain mutant mice (Revest et al., 2001; Sun et al., 2002), it was not observed in the proximal mesenchyme of *Fgfr2*$^{\text{AER-KO}}$ forelimbs,

as reported here and by a recent study (Yu and Ornitz, 2008). These differences in the cell death patterns, in addition to the final skeletal phenotypes, are due to the fact that AER-FGF signaling is reduced earlier and/or more greatly in limb buds where AER fails to initiate (Revest et al., 2001) or in limb buds where AER-*Fgf4*/*8* are directly ablated (Sun et al., 2002) than in *Fgfr2*$^{AER-KO}$ forelimb buds, where AER-*Fgf* is, although progressively less, continuously expressed until the 45 s stage. Together, these data suggest that AER function is required for the survival of stylopod and zeugopod progenitors, but not of autopod progenitors.

Interestingly, our analyses detected no significant differences of cell proliferation in the distal mesenchyme between mutant and control limb buds. These data thus join several previous studies, which also show that cell proliferation is not affected in mutant limb buds that fail to form skeletal elements, including the autopod (Barrow et al., 2003; Revest et al., 2001; Sun et al., 2002; Verheyden et al., 2005). Furthermore, it was observed over three decades ago (Janners and Searls, 1971) that cell proliferation is unchanged after AER removal in chicken limb buds. Taken together, these results support our conclusion that reduced cell proliferation in the distal mesenchyme is unlikely to account for loss of the distal autopod. Finally, although the lack of abnormal cell death and cell proliferation in the distal mesenchyme led us to discovering AER function in generation of distal limb progenitors, we do not exclude the possibility that, earlier, the AER may also regulate cell proliferation of the distal progenitors.

FGFR2 and Wnt/β-catenin signaling interact to maintain the AER

Previous studies have shown that the FGF10-FGF8 loop, presumably via ectodermal FGFR2, operates to initiate the AER during vertebrate limb development (Crossley et al., 1996; Ohuchi et al., 1997). It was further suggested that FGF10 may be the ‘AER maintenance factor’ in the posterior limb mesenchyme to maintain AER morphology (Ohuchi et al., 1997). In this study, by conditionally removing FGFR2 function, we demonstrate that loss of *Fgfr2* function causes failure of AER maintenance and, as a consequence, loss of the forelimb autopod. Our results therefore support the model that FGFR2 signaling maintains the AER after AER initiation.

Msx2-cre-mediated loss of *Fgfr2* function in the AER and ventral ectoderm increased cell death in these tissues, where both *Fgfr2* and the *cre* transgene are expressed. These results suggest that FGFR2 acts as a survival factor to maintain the AER. Interestingly, cell death is also increased in limb ectoderm of mice lacking *Fgfr2b* function, in which the AER fails to initiate (Revest et al., 2001). Thus, these results suggest that FGFR2 promotes cell survival in both AER initiation and maintenance during limb development.

Several lines of evidence indicate that FGFR2 interacts with Wnt/β-catenin signaling during AER maintenance. Wnt/β-catenin signaling activities, as measured by β-Gal staining using the BAT-Gal transgene, are greatly reduced in the AER of *Fgfr2*$^{AER-KO}$ limb buds. Expression of *Lef1*, which together with *Tcf1* is required for AER initiation, is also downregulated in mutant limb buds. Furthermore, loss of β-catenin (Barrow et al., 2003) and FGFR2 function via *Msx2-cre* cause similar patterns of cell death increase in the forelimb ectoderm, suggesting that they interact to promote cell survival during AER maintenance. Finally, a gain of Wnt/β-catenin signaling rescues AER loss and this in turn restores the autopod bones missing in *Fgfr2*$^{AER-KO}$ limbs. FGF signaling interacts with Wnt/β-catenin signaling during early limb bud development (Barrow et al., 2003; Galceran et al., 1999). Together with our data, these studies suggest that interactions of FGF and Wnt/β-catenin signaling pathways are required at multiple stages of vertebrate limb development.

Acknowledgements

We thank J. C. Belmonte, D. Duboule, R. Harland, J. Hébert, J. Helms, J. Innis, N. Itoh, A. Joyner, V. Lefebvre, A. McMahon, D. Ornitz, J. Rubenstein and J. Wozney for providing plasmids from which the probes for in situ

hybridization were made. We thank Helen Capili for excellent technical assistance, and Gary Freeman, Sylvain Provot and Mimi Zeiger for critical reading of the manuscript. Supported by an NIH NRSA HL07731 (P.L.) and NIH grants AR046238 and CA057621 (Z.W.).

References

Ahn K, Mishina Y, Hanks MC, Behringer RR, Crenshaw EB 3rd. BMPR-IA signaling is required for the formation of the apical ectodermal ridge and dorsal-ventral patterning of the limb. Development 2001;128:4449–4461. [PubMed: 11714671]

Altabef M, Clarke JD, Tickle C. Dorso-ventral ectodermal compartments and origin of apical ectodermal ridge in developing chick limb. Development 1997;124:4547–4556. [PubMed: 9409672]

Arman E, Haffner-Krausz R, Chen Y, Heath JK, Lonai P. Targeted disruption of fibroblast growth factor (FGF) receptor 2 suggests a role for FGF signaling in pregastrulation mammalian development. Proc Natl Acad Sci USA 1998;95:5082–5087. [PubMed: 9560232]

Arman E, Haffner-Krausz R, Gorivodsky M, Lonai P. Fgfr2 is required for limb outgrowth and lung-branching morphogenesis. Proc Natl Acad Sci USA 1999;96:11895–11899. [PubMed: 10518547]

Barrow JR, Thomas KR, Boussadia-Zahui O, Moore R, Kemler R, Capecchi MR, McMahon AP. Ectodermal Wnt3/beta-catenin signaling is required for the establishment and maintenance of the apical ectodermal ridge. Genes Dev 2003;17:394–409. [PubMed: 12569130]

Capdevila J, Izpisua Belmonte JC. Patterning mechanisms controlling vertebrate limb development. Annu Rev Cell Dev Biol 2001;17:87–132. [PubMed: 11687485]

Coumoul X, Shukla V, Li C, Wang RH, Deng CX. Conditional knockdown of Fgfr2 in mice using Cre-LoxP induced RNA interference. Nucleic Acids Res 2005;33:e102. [PubMed: 15987787]

Crossley PH, Minowada G, MacArthur CA, Martin GR. Roles for FGF8 in the induction, initiation, and maintenance of chick limb development. Cell 1996;84:127–136. [PubMed: 8548816]

De Moerlooze L, Spencer-Dene B, Revest J, Hajihosseini M, Rosewell I, Dickson C. An important role for the IIIb isoform of fibroblast growth factor receptor 2 (FGFR2) in mesenchymal-epithelial signalling during mouse organogenesis. Development 2000;127:483–492. [PubMed: 10631169]

Dudley AT, Ros MA, Tabin CJ. A re-examination of proximodistal patterning during vertebrate limb development. Nature 2002;418:539–544. [PubMed: 12152081]

Fromental-Ramain C, Warot X, Messadecq N, LeMeur M, Dolle P, Chambon P. Hoxa-13 and Hoxd-13 play a crucial role in the patterning of the limb autopod. Development 1996;122:2997–3011. [PubMed: 8898214]

Galceran J, Farinas I, Depew MJ, Clevers H, Grosschedl R. Wnt3a−/−like phenotype and limb deficiency in Lef1(−/−)Tcf1(−/−) mice. Genes Dev 1999;13:709–717. [PubMed: 10090727]

Gorivodsky M, Lonai P. Novel roles of Fgfr2 in AER differentiation and positioning of the dorsoventral limb interface. Development 2003;130:5471–5479. [PubMed: 14507786]

Guo Q, Loomis C, Joyner AL. Fate map of mouse ventral limb ectoderm and the apical ectodermal ridge. Dev Biol 2003;264:166–178. [PubMed: 14623239]

Harada N, Tamai Y, Ishikawa T, Sauer B, Takaku K, Oshima M, Taketo MM. Intestinal polyposis in mice with a dominant stable mutation of the beta-catenin gene. EMBO J 1999;18:5931–5942. [PubMed: 10545105]

Hashimoto K, Yokouchi Y, Yamamoto M, Kuroiwa A. Distinct signaling molecules control Hoxa-11 and Hoxa-13 expression in the muscle precursor and mesenchyme of the chick limb bud. Development 1999;126:2771–2783. [PubMed: 10331987]

Itoh N, Ornitz DM. Evolution of the Fgf and Fgfr gene families. Trends Genet 2004;20:563–569. [PubMed: 15475116]

Janners MY, Searls RL. Effect of removal of the apical ectodermal ridge on the rate of cell division in the subridge mesenchyme of the embryonic chick wing. Dev Biol 1971;24:465–476. [PubMed: 5578887]

Kawakami Y, Capdevila J, Buscher D, Itoh T, Rodriguez Esteban C, Izpisua Belmonte JC. WNT signals control FGF-dependent limb initiation and AER induction in the chick embryo. Cell 2001;104:891–900. [PubMed: 11290326]

Kawakami Y, Rodriguez-Leon J, Koth CM, Buscher D, Itoh T, Raya A, Ng JK, Esteban CR, Takahashi S, Henrique D, et al. MKP3 mediates the cellular response to FGF8 signalling in the vertebrate limb. Nat Cell Biol 2003;5:513–519. [PubMed: 12766772]

Kengaku M, Capdevila J, Rodriguez-Esteban C, De La Pena J, Johnson RL, Belmonte JC, Tabin CJ. Distinct WNT pathways regulating AER formation and dorsoventral polarity in the chick limb bud. Science 1998;280:1274–1277. [PubMed: 9596583]

Kimmel RA, Turnbull DH, Blanquet V, Wurst W, Loomis CA, Joyner AL. Two lineage boundaries coordinate vertebrate apical ectodermal ridge formation. Genes Dev 2000;14:1377–1389. [PubMed: 10837030]

Lewandoski M, Sun X, Martin GR. Fgf8 signalling from the AER is essential for normal limb development. Nat Genet 2000;26:460–463. [PubMed: 11101846]

Li C, Xu X, Nelson DK, Williams T, Kuehn MR, Deng CX. FGFR1 function at the earliest stages of mouse limb development plays an indispensable role in subsequent autopod morphogenesis. Development 2005;132:4755–4764. [PubMed: 16207751]

Loomis C, Kimmel R, Tong C, Michaud J, Joyner A. Analysis of the genetic pathway leading to formation of ectopic apical ectodermal ridges in mouse Engrailed-1 mutant limbs. Development 1998;125:1137–1148. [PubMed: 9463360]

Lu P, Minowada G, Martin GR. Increasing Fgf4 expression in the mouse limb bud causes polysyndactyly and rescues the skeletal defects that result from loss of Fgf8 function. Development 2006;133:33–42. [PubMed: 16308330]

Maretto S, Cordenonsi M, Dupont S, Braghetta P, Broccoli V, Hassan AB, Volpin D, Bressan GM, Piccolo S. Mapping Wnt/beta-catenin signaling during mouse development and in colorectal tumors. Proc Natl Acad Sci USA 2003;100:3299–3304. [PubMed: 12626757]

Mariani FV, Martin GR. Deciphering skeletal patterning: clues from the limb. Nature 2003;423:319–325. [PubMed: 12748649]

Martin GR. The roles of FGFs in the early development of vertebrate limbs. Genes Dev 1998;12:1571–1586. [PubMed: 9620845]

Mercader N, Leonardo E, Piedra ME, Martinez AC, Ros MA, Torres M. Opposing RA and FGF signals control proximodistal vertebrate limb development through regulation of Meis genes. Development 2000;127:3961–3970. [PubMed: 10952894]

Min H, Danilenko DM, Scully SA, Bolon B, Ring BD, Tarpley JE, DeRose M, Simonet WS. Fgf-10 is required for both limb and lung development and exhibits striking functional similarity to Drosophila branchless. Genes Dev 1998;12:3156–3161. [PubMed: 9784490]

Moon AM, Capecchi MR. Fgf8 is required for outgrowth and patterning of the limbs. Nat Genet 2000;26:455–459. [PubMed: 11101845]

Nelson CE, Morgan BA, Burke AC, Laufer E, DiMambro E, Murtaugh LC, Gonzales E, Tessarollo L, Parada LF, Tabin C. Analysis of Hox gene expression in the chick limb bud. Development 1996;122:1449–1466. [PubMed: 8625833]

Niswander L. Pattern formation: old models out on a limb. Nat Rev Genet 2003;4:133–143. [PubMed: 12560810]

Niswander L, Tickle C, Vogel A, Booth I, Martin GR. FGF-4 replaces the apical ectodermal ridge and directs outgrowth and patterning of the limb. Cell 1993;75:579–587. [PubMed: 8221896]

Ohuchi H, Nakagawa T, Yamamoto A, Araga A, Ohata T, Ishimaru Y, Yoshioka H, Kuwana T, Nohno T, Yamasaki M, et al. The mesenchymal factor, FGF10, initiates and maintains the outgrowth of the chick limb bud through interaction with FGF8, an apical ectodermal factor. Development 1997;124:2235–2244. [PubMed: 9187149]

Pizette S, Niswander L. BMPs negatively regulate structure and function of the limb apical ectodermal ridge. Development 1999;126:883–894. [PubMed: 9927590]

Revest JM, Spencer-Dene B, Kerr K, De Moerlooze L, Rosewell I, Dickson C. Fibroblast growth factor receptor 2-IIIb acts upstream of Shh and Fgf4 and is required for limb bud maintenance but not for the induction of Fgf8, Fgf10, Msx1, or Bmp4. Dev Biol 2001;231:47–62. [PubMed: 11180951]

Sato K, Koizumi Y, Takahashi M, Kuroiwa A, Tamura K. Specification of cell fate along the proximal-distal axis in the developing chick limb bud. Development 2007;134:1397–1406. [PubMed: 17329359]

Saunders JW Jr. The proximo-distal sequence of the origin of the parts of the chick wing and the role of the ectoderm. J Exp Zool 1948;108:363–403. [PubMed: 18882505]

Sekine K, Ohuchi H, Fujiwara M, Yamasaki M, Yoshizawa T, Sato T, Yagishita N, Matsui D, Koga Y, Itoh N, et al. Fgf10 is essential for limb and lung formation. Nat Genet 1999;21:138–141. [PubMed: 9916808]

Sherman L, Wainwright D, Ponta H, Herrlich P. A splice variant of CD44 expressed in the apical ectodermal ridge presents fibroblast growth factors to limb mesenchyme and is required for limb outgrowth. Genes Dev 1998;12:1058–1071. [PubMed: 9531542]

Summerbell D. A quantitative analysis of the effect of excision of the AER from the chick limb bud. J Embryol Exp Morphol 1974;32:651–660. [PubMed: 4463222]

Summerbell D, Lewis JH, Wolpert L. Positional information in chick limb morphogenesis. Nature 1973;244:492–496. [PubMed: 4621272]

Sun X, Lewandoski M, Meyers EN, Liu YH, Maxson RE Jr, Martin GR. Conditional inactivation of Fgf4 reveals complexity of signalling during limb bud development. Nat Genet 2000;25:83–86. [PubMed: 10802662]

Sun X, Mariani FV, Martin GR. Functions of FGF signalling from the apical ectodermal ridge in limb development. Nature 2002;418:501–508. [PubMed: 12152071]

Tabin C, Wolpert L. Rethinking the proximodistal axis of the vertebrate limb in the molecular era. Genes Dev 2007;21:1433–1442. [PubMed: 17575045]

Tarchini B, Duboule D. Control of Hoxd genes' collinearity during early limb development. Dev Cell 2006;10:93–103. [PubMed: 16399081]

Vargesson N, Clarke JD, Vincent K, Coles C, Wolpert L, Tickle C. Cell fate in the chick limb bud and relationship to gene expression. Development 1997;124:1909–1918. [PubMed: 9169838]

Vargesson N, Kostakopoulou K, Drossopoulou G, Papageorgiou S, Tickle C. Characterisation of hoxa gene expression in the chick limb bud in response to FGF. Dev Dyn 2001;220:87–90. [PubMed: 11146510]

Verheyden JM, Lewandoski M, Deng C, Harfe BD, Sun X. Conditional inactivation of Fgfr1 in mouse defines its role in limb bud establishment, outgrowth and digit patterning. Development 2005;132:4235–4245. [PubMed: 16120640]

Wolpert L, Tickle C, Sampford M. The effect of cell killing by x-irradiation on pattern formation in the chick limb. J Embryol Exp Morphol 1979;50:175–193. [PubMed: 458354]

Xu X, Weinstein M, Li C, Naski M, Cohen R, Ornitz D, Leder P, Deng C. Fibroblast growth factor receptor 2 (FGFR2)-mediated reciprocal regulation loop between FGF8 and FGF10 is essential for limb induction. Development 1998;125:753–765. [PubMed: 9435295]

Yu K, Ornitz DM. FGF signaling regulates mesenchymal differentiation and skeletal patterning along the limb bud proximodistal axis. Development 2008;135:483–491. [PubMed: 18094024]

Yu K, Xu J, Liu Z, Sosic D, Shao J, Olson EN, Towler DA, Ornitz DM. Conditional inactivation of FGF receptor 2 reveals an essential role for FGF signaling in the regulation of osteoblast function and bone growth. Development 2003;130:3063–3074. [PubMed: 12756187]

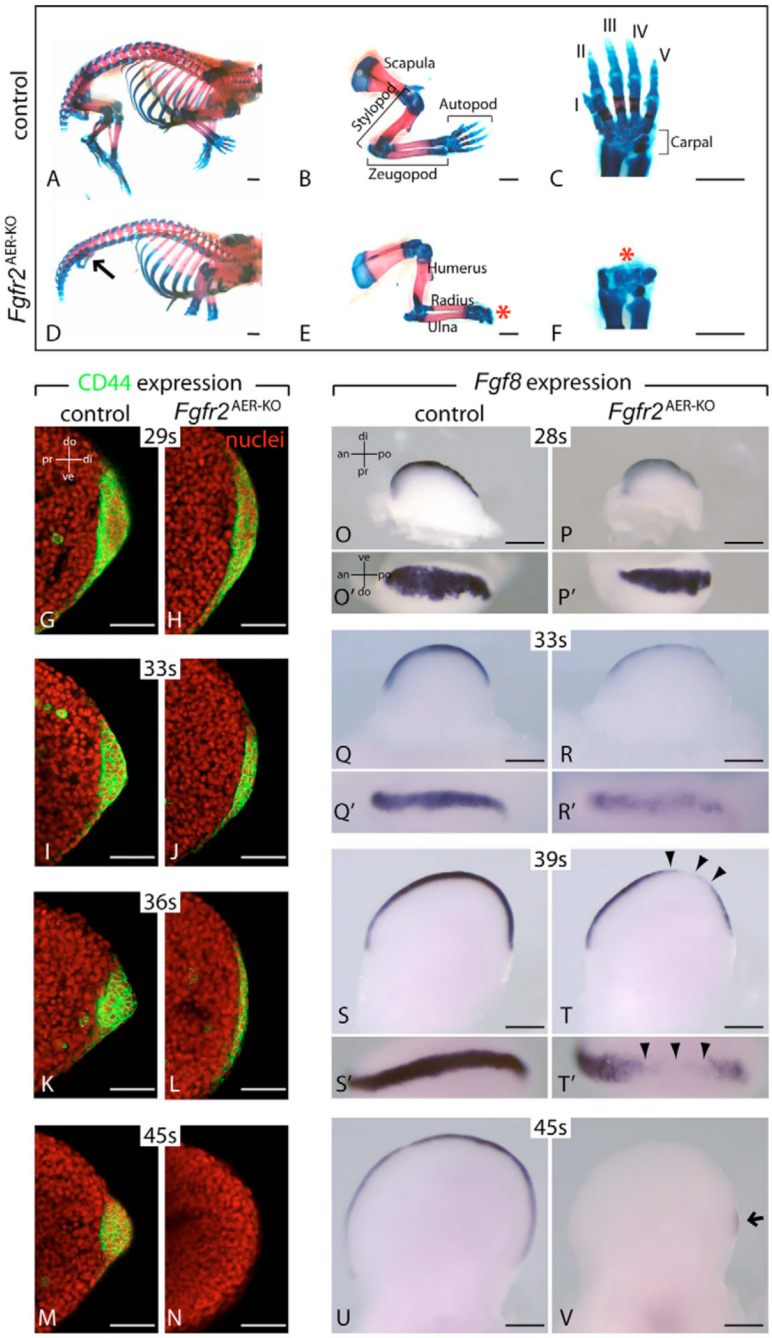

Fig. 1. Fgfr2 removal causes loss of the apical ectodermal ridge (AER), reduction of AER-FGF and loss of distal limb skeletal elements. (A–F)

Skeletal preparations of E18.5 embryos, with cartilage stained blue and bone stained red. In *Fgfr2*$^{\text{AER-KO}}$ embryos, the hindlimb was missing except for the pelvic bones (arrow in D) and the distal autopod (hand-plate) was absent in the forelimb (asterisk in E, F; *n*=18). Individual digits in control embryos are numbered I–V, from anterior to posterior (C). Scale bars: 1 mm. (**G–N**) AER histology as examined by CD44 immunofluorescence (green) on vibratome sections. Samples were counterstained with a nuclear dye To-Pro3 (red). Scale bars: 50 μm. (**O–V**) Levels of AER-*Fgf8* expression as detected by whole-mount RNA in situ hybridization assays at the stages indicated. *Fgf8*-expressing cells were sparser in the mutant AER (R, R′)

than in the control AER (Q, Q′) at the 33 s stage. Black arrowheads indicate gaps in the AER that lack *Fgf8* expression in the mutant limb buds (T, T′). Arrow indicates a small patch of the limb bud edge that was still expressing *Fgf8* (V). Scale bars: 200 μm. Abbreviations: an, anterior; di, distal; do, dorsal; pr, proximal; po, posterior; ve, ventral; s, somite.

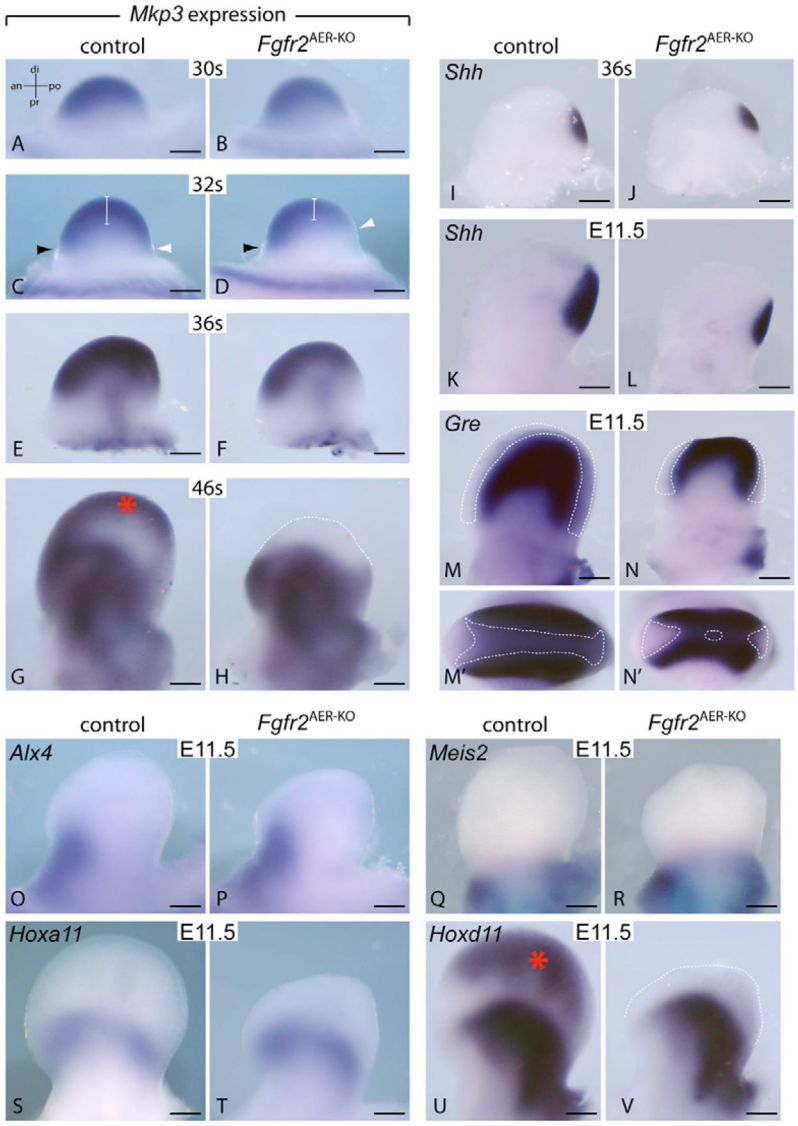

Fig. 2. Altered expression of key mesenchymal patterning genes in *Fgfr2*$^{AER-KO}$ forelimb buds

(**A–V**) Whole-mount RNA in situ hybridization assays for the genes indicated. (A–H) *Mkp3* expression as a read-out of mesenchymal responses to AER-FGFs. Vertical white lines in C, D indicate the depth of *Mkp3*-positive domain with black and white arrowheads marking the anterior and posterior boundaries, respectively. Asterisk indicates the *Mkp3* expression domain in the sub-AER mesenchyme that was absent in the mutant limb bud (dotted line, H). (I–N′) Expression of *Shh* (I–L) and *Gre* (M–N′). The distal strip of sub-AER mesenchyme (broken white lines), which lacks *Gre* expression, was much smaller in mutant forelimb buds. (M′, N ′) The strip outlined by broken white lines, indicating the *Gre*-negative middle section of the LBM was greatly reduced in mutant limb buds at E11.5 (N′). (O–V) Expression of genes that primarily mark the anterior (*Alx4*;O, P), proximal (*Meis2*; Q, R) and middle mesenchyme (*Hoxa11*; S, T) and *Hoxd11* expression (U, V) at E11.5. There are two distinct domains of *Hoxd11* expression, marking the proximal and distal (*) mesenchyme. The distal domain of *Hoxd11* expression, which gives rise to the autopod, was missing in the mutant limb (broken lines in V). E11.5 is equivalent to ~the 45 s stage. Scale bars: 200 μm. Abbreviations: an, anterior; di, distal; do, dorsal; pr, proximal; po, posterior; ve, ventral; s, somite.

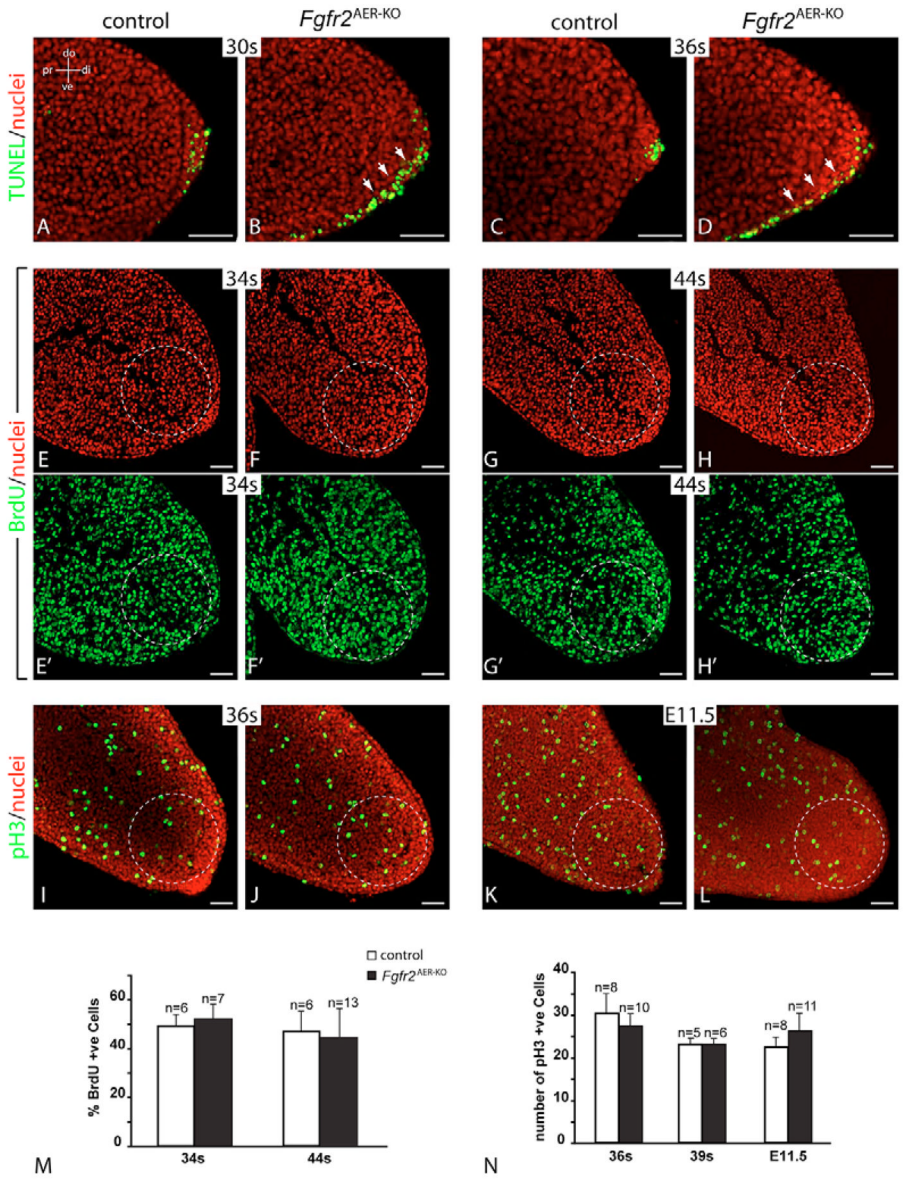

Fig. 3. Normal cell death and cell proliferation in the distal mesenchyme of *Fgfr2*$^{AER\text{-}KO}$ forelimb buds

(**A–D**) Cell death as detected by TUNEL assay (green) at the stages indicated. Note that there were more dying cells in the AER and ventral ectoderm of mutant forelimb buds than in controls at the 30 s (B; *n*=6) and the 36 s (D; *n*=6) stages. (**E–L**) Cell proliferation as detected via BrdU incorporation (E–H′, M) and pH3 immunofluorescence (I–L, N), which marks nuclei in cells undergoing mitosis, in the forelimb buds of mutant and control embryos. White circles indicate the areas (φ=200 μm) of sub-AER mesenchyme in which BrdU- (**M**) or pH3- (**N**) positive cells were quantified. Values are the mean±s.d. for each data point in M and the mean±s.e.m. for each data point in N. No statistically significant differences in the percentage of BrdU-positive cells or in the number of pH3-positive cells were observed between the control and mutant limb buds at the stages indicated (unpaired, two-tailed Student's *t*-test). E11.5 is equivalent to ~45 s stage. Scale bars: 50 μm. Abbreviations: an, anterior; di, distal; do, dorsal; pr, proximal; po, posterior; ve, ventral; s, somite.

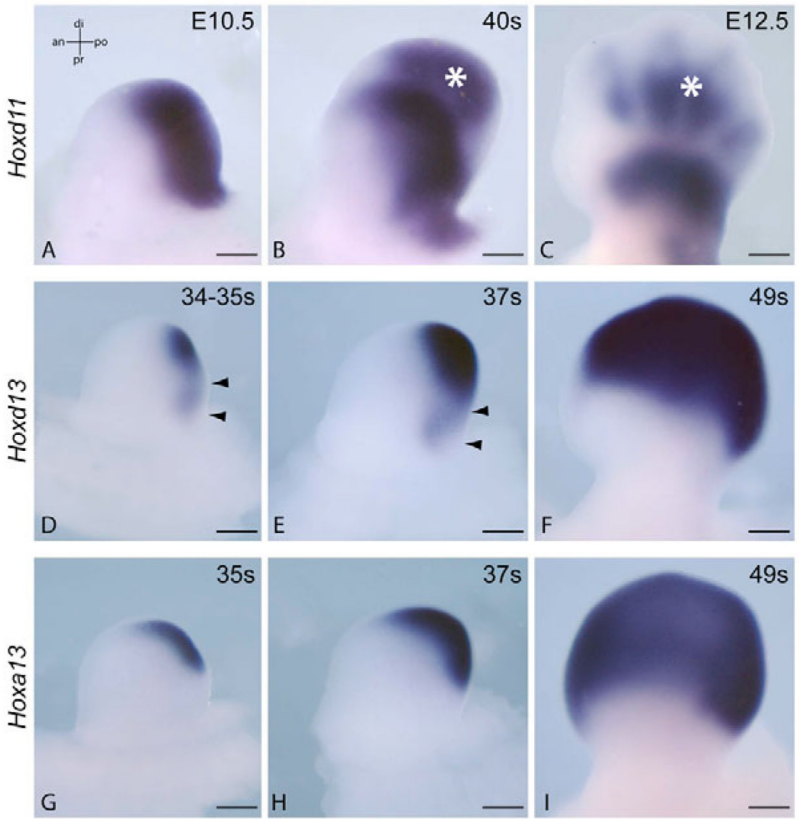

Fig. 4. Expression of *Hoxd11*, *Hoxd13* and *Hoxa13* in early mouse limb buds

(A–I) Whole-mount in situ hybridization assays for *Hoxd11*, *Hoxd13* and *Hoxa13* expression in normal forelimb buds. (**A–C**) *Hoxd11* expression. Its distal domain (asterisk) in the posterior-distal autopod (B, C) marks the future autopod at E12.5 (C). (**D–F**) *Hoxd13* expression. The proximal domain of *Hox13* expression (arrowheads) at the 34–35 s stage was gradually lost over time. (**G–I**) *Hoxa13* expression at the stages indicated. E10.5 is equivalent to ~35 s stage. Scale bars: 200 μm. Abbreviations: an, anterior; di, distal; do, dorsal; pr, proximal; po, posterior; ve, ventral; s, somite.

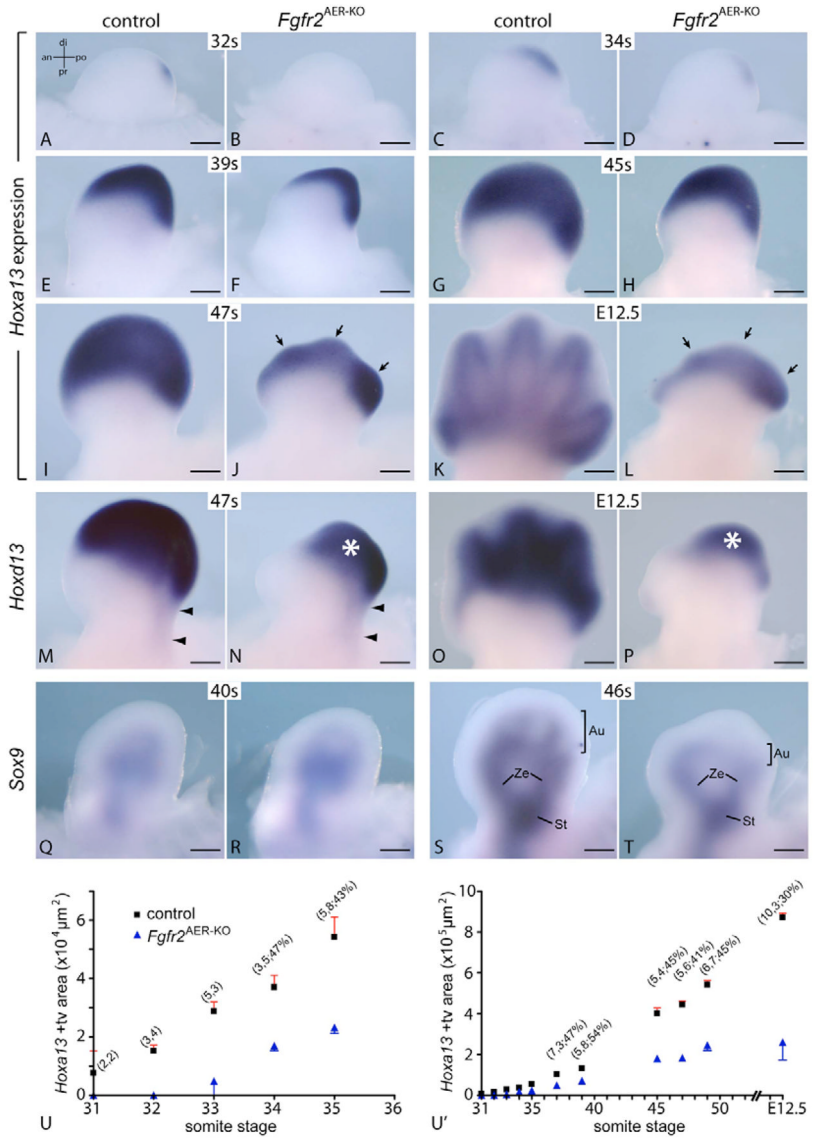

Fig. 5. Delayed generation of autopod progenitors in *Fgfr2*$^{AER-KO}$ forelimbs

(**A–T**) Whole-mount in situ hybridization assays for *Hoxa13*, *Hoxd13* and *Sox9* expression. (A–L) Generation and expansion of autopod progenitors as indicated by *Hoxa13* expression. *Hoxa13* expression was delayed by 2 s stages in the mutant. The outline of mutant limb buds changed between the 45 s (H) and 47 s (J) stages, coinciding with the onset of autopod condensation (S, T). (M–P) *Hoxd13* expression in the distal autopod. Asterisk in N, P indicates residual *Hoxd13* expression in mutant limb buds. The proximal domain of *Hoxd13* expression (arrowheads) was present in control (M) and mutant limb buds (N) at the 47 s stage. (Q–T) Skeletal progenitors at the 40 s and 46 s stages as marked by *Sox9* expression. Skeletal condensation of the autopod, yet to start at the 40 s stage (Q, R), occurred by the 46 s stage as indicated by primitive limb elements (S). (**U**, **U′**) Quantification of the area of *Hoxa13*-expression domain during autopod development. Values in parentheses at each data point are the numbers of control and mutant samples examined, and the percentage of the area of *Hoxa13*-expression domain in the mutant compared with that in the control. Values are the

mean±s.d. for each data point in U, U′. Scale bars: 200 μm. Abbreviations: an, anterior; Au, autopod; di, distal; po, posterior; pr, proximal; s, somite; St, stylopod; Ze, zeugopod.

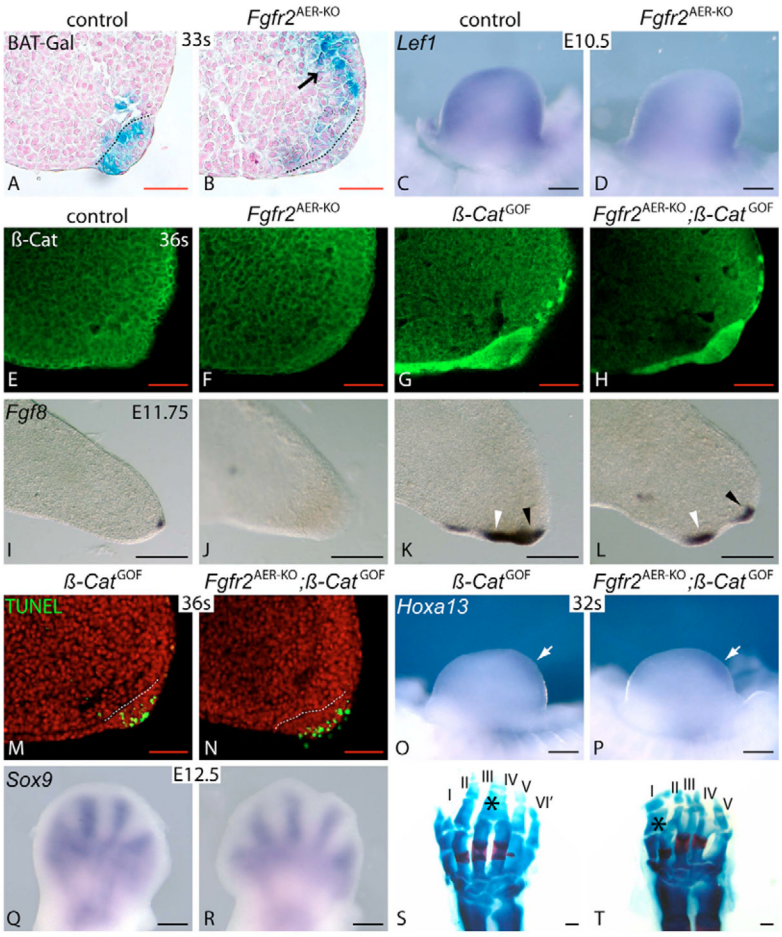

Fig. 6. FGFR2 interacts with Wnt/β-catenin signaling to maintain the AER

(**A–D**) Reduction of Wnt/β-catenin signaling in *Fgfr2*$^{AER\text{-}KO}$ forelimb buds. (A, B) *lacZ* expression in BAT-Gal transgenic limb buds. Broken black lines mark the basement membrane. Arrow in B denotes ectopic Wnt signaling in the distal-dorsal mesenchyme. (C, D) *Lef1* expression was moderately reduced in mutant limb buds. (**E–T**) β-Catenin^{GOF} prevented premature AER loss and restored the autopod of *Fgfr2*$^{AER\text{-}KO}$ embryos. (E–H) β-Catenin expression immunofluorescence. Stabilized β-catenin was present in the ventral ectoderm. (I–L) *Fgf8* expression on vibratome sections. Ectopic *Fgf8*-expression in the ventral ectoderm (white arrowheads). Black arrowheads indicate the endogenous AER (K, L). (M, N) Cell death as detected by TUNEL. Dying cells in the ventral ectoderm, which were prominent in *Fgfr2*$^{AER\text{-}KO}$ limb buds, were absent in *Fgfr2*$^{AER\text{-}KO}$; *β-cat*^{GOF} limb buds at this stage (Fig. 3D). Broken white lines indicate the basement-membrane. (O, P) *Hoxa13* expression (white arrow) was initiated in *β-cat*^{GOF} limb buds at 32 s. (Q–T) *Sox9* expression and skeletal preparations at the stages indicated. Note that the autopod was restored in *Fgfr2*$^{AER\text{-}KO}$; *β-cat*^{GOF} embryos (R, T). Asterisk indicates skeletal fusions between digits (syndactyly) in *β-cat*^{GOF} (S) and *Fgfr2*$^{AER\text{-}KO}$; *β-cat*^{GOF} limbs (T). VI′ indicates a post-axial extra digit (S). E10.5 is equivalent to ~35 s stage and E11.75 is equivalent to ~48 s stage. Scale bars: red, 50 μm; black, 200 μm. Abbreviations: an, anterior; di, distal; do, dorsal; pr, proximal; po, posterior; ve, ventral; s, somite.

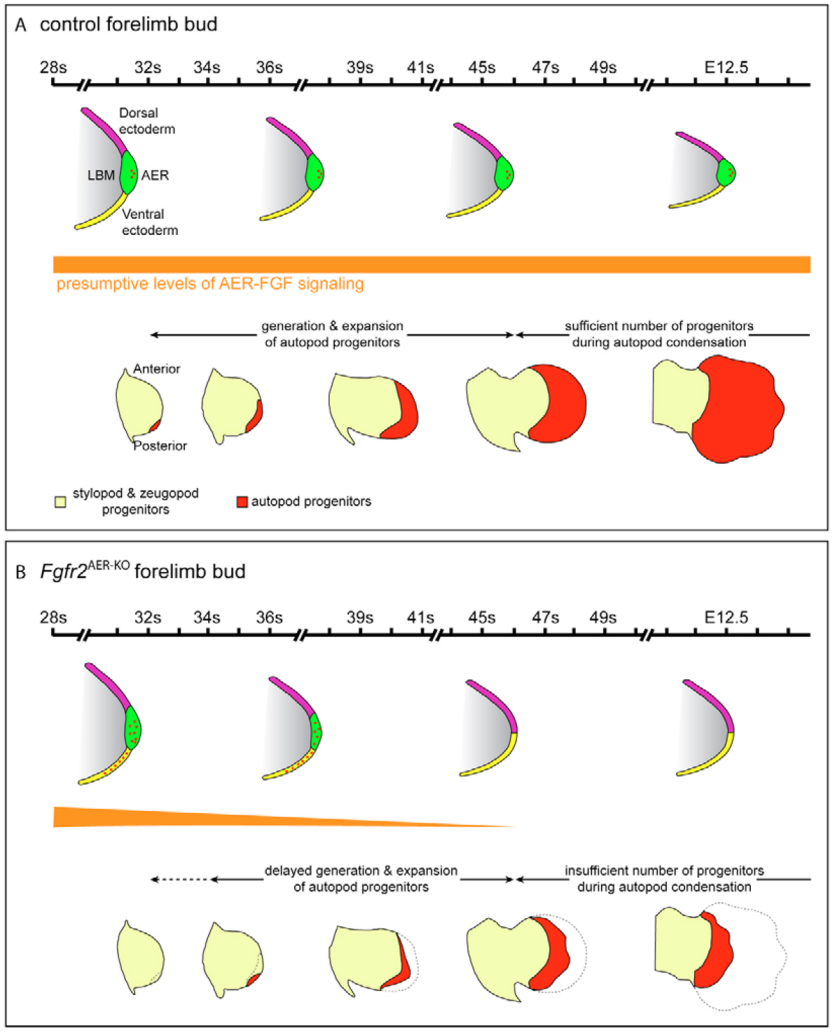

Fig. 7. A model of AER function in development of the mouse forelimb autopod

(**A**, **B**) AER maintenance is essential for AER-FGF signaling and generation of autopod progenitors. Schematic diagrams of early limb buds in transverse views (top row in A, B) and whole-mount dorsal views (bottom row in A, B) to illustrate development of the AER (green) and autopod progenitors, as marked by *Hoxa13* expression (red). Red dots indicate dying cells in the ventral ectoderm and AER. (A) In control forelimb buds, the AER is maintained and AER-FGF production (orange) is normal. As a result, FGF signaling in the distal limb bud mesenchyme (LBM) is sustained and autopod progenitors are generated at the 31–32 s stage. The progenitor pool expands subsequently and a sufficient number of skeletal progenitors are available to form a normal autopod when condensation starts at around the 46 s stage. (B) In *Fgfr2*$^{\text{AER-KO}}$ forelimb buds, the AER is not maintained because of increased cell death and AER-FGF production progressively decreases. As a result, FGF signaling in the distal mesenchyme is reduced and generation of autopod progenitors is delayed by 2-somite stages until the 33–34 s stage. Although the progenitor pool expands grossly normally at later stages, it fails to produce a sufficient number of skeletal progenitors to form a normal autopod at the onset of autopod condensation.

Table 1

Stage specificity of *Hoxa13* expression in early forelimb buds

Stage	Control	*Fgfr2*$^{AER-KO}$	*β-catenin*^{GOF}	*Fgfr2*$^{AER-KO}$;*β-catenin*^{GOF}
30 somites	0/2	0/3	n.d.	n.d.
31 somites	1/2	0/2	0/2	0/4
32 somites	3/3*	0/4*	2/2†	5/5†
33 somites	5/5	1/3	n.d.	n.d.
34 somites	3/3*	5/5*	1/1	2/2
35 somites	5/5	8/8	3/3	2/2

Hoxa13 expression was detected by whole-mount in situ hybridization. Numerator and denominator indicate the number of embryos positive for *Hoxa13* expression and the number examined, respectively, at the stages indicated. Abbreviation: n.d. not determined.

* Shown in Fig. 5.

† Shown in Fig. 6.